


RESEARCH

Open Access



Activation of GPR40 attenuates neuroinflammation and improves neurological function via PAK4/CREB/KDM6B pathway in an experimental GMH rat model

Jie Xiao^{1,2}, Tao Cai³, Yuanjian Fang², Rui Liu², Jerry J. Flores², Wenna Wang², Ling Gao², Yu Liu², Qin Lu², Lihui Tang², John H. Zhang^{2,4}, Hongwei Lu^{5*} and Jiping Tang^{2*} 

Abstract

Background: Germinal matrix hemorrhage (GMH) is defined by the rupture of immature blood vessels in the germinal matrix, where subsequent hemorrhage enters the subependymal zone and the cerebral lateral ventricles. The consequent blood clot has been identified as the causative factor of secondary brain injury, which triggers a series of complex parallel and sequential harmful mechanisms, including neuroinflammation. The orphan G-protein-coupled receptor 40 (GPR40), a free fatty acid (FFA) receptor 1, has been shown to exert anti-inflammatory effects when activated and improved outcomes in animal models of stroke. We aimed to investigate the anti-inflammatory effects of GPR40 and its underlying mechanisms after GMH.

Methods: GMH model was induced in 7-day-old rat pups by an intraparenchymal injection of bacterial collagenase. GPR40 agonist, GW9508, was administered intranasally 1 h, 25 h, and 49 h after GMH induction. CRISPR targeting GPR40, PAK4, and KDM6B were administered through intracerebroventricular injection 48 h before GMH induction. Neurologic scores, microglia polarization, and brain morphology were evaluated by negative geotaxis, right reflex, rotarod test, foot fault test, Morris water maze, immunofluorescence staining, Western blots, and nissl staining respectfully.

* Correspondence: hongweilu@csu.edu.cn; jtang@llu.edu

⁵Center for Experimental Medicine, The Third Xiangya Hospital of Central South University, 138 Tongzipo Road, Changsha, Hunan 410013, People's Republic of China

²Department of Physiology and Pharmacology, Loma Linda University School of Medicine, Loma Linda, California 92354, USA

Full list of author information is available at the end of the article



© The Author(s). 2021 **Open Access** This article is licensed under a Creative Commons Attribution 4.0 International License, which permits use, sharing, adaptation, distribution and reproduction in any medium or format, as long as you give appropriate credit to the original author(s) and the source, provide a link to the Creative Commons licence, and indicate if changes were made. The images or other third party material in this article are included in the article's Creative Commons licence, unless indicated otherwise in a credit line to the material. If material is not included in the article's Creative Commons licence and your intended use is not permitted by statutory regulation or exceeds the permitted use, you will need to obtain permission directly from the copyright holder. To view a copy of this licence, visit <http://creativecommons.org/licenses/by/4.0/>. The Creative Commons Public Domain Dedication waiver (<http://creativecommons.org/publicdomain/zero/1.0/>) applies to the data made available in this article, unless otherwise stated in a credit line to the data.

Results: The results demonstrated that GW9508 improved neurological and morphological outcomes after GMH in the short (24 h, 48 h, 72h) and long-term (days 21–27). However, the neuroprotective effects of treatment were abolished by GW1100, a selective GPR40 antagonist. GW9508 treatment increased populations of M2 microglia and decreased M1 microglia in periventricular areas 24 h after GMH induction. GW9508 upregulated the phosphorylation of PAK4, CREB, and protein level of KDM6B, CD206, IL-10, which was also met with the downregulation of inflammatory markers IL-1 β and TNF- α . The mechanism study demonstrated that the knockdown of GPR40, PAK4, and KDM6B reversed the neuroprotective effects brought on by GW9508. This evidence suggests that GPR40/PAK4/CREB/KDM6B signaling pathway in microglia plays a role in the attenuation of neuroinflammation after GMH.

Conclusions: In conclusion, the present study demonstrates that the activation of GPR40 attenuated GMH-induced neuroinflammation through the activation of the PAK4/CREB/KDM6B signaling pathway, and M2 microglia may be a major mediator of this effect. Thus, GPR40 may serve as a potential target in the reduction of the inflammatory response following GMH, thereby improving neurological outcomes in the short- and long-term.

Keywords: GPR40, Germinal matrix hemorrhage, Microglia, Neuroinflammation

Background

Germinal matrix hemorrhage (GMH) is the most common neurological disorder of preterm infants, which is associated with a high rate of disability and mortality [1]. GMH results from the rupture of immature blood vessels in the subependymal tissue that leads to primary and secondary brain injury, which results in hydrocephalus, epilepsy, and developmental delay [2]. Microglia have been attributed to play a primary role in the mediation of neuroinflammation, which has been shown to contribute to post-hemorrhagic tissue destruction causing morphological and functional impairments [3]. Therefore, the inhibition of the neuroinflammation could be a potential therapeutic strategy for patients with GMH.

Microglia are resident macrophages of the central nervous system, which have been shown to contribute to the acute inflammatory response after GMH and other hemorrhagic brain diseases [4, 5]. After brain hemorrhage, microglia cells are activated and polarized into two distinct phenotypes which are defined as the classically activated (M1) phenotype and the alternatively activated microglia (M2) phenotype [6]. M1 phenotypic microglia have been shown to be pro-inflammatory, where the production of inflammatory cytokines (e.g., IL-1 β , IL-12, tumor necrosis factor- α (TNF- α)) have shown to cause brain injury [7]. By contrast, M2 phenotypic microglia contribute to CNS repair, as various studies have demonstrated that M2 microglia play a vital role in the clearance of cell debris, resolution inflammation, the phagocytosis of RBC, and releases a plethora of trophic factors to promote brain recovery (e.g., IL-10, Arginase 1, CD206, Ym1, Fizz1) [8–13]. Therefore, the polarization of microglia from M1 to M2 state may provide a potential therapy for GMH.

G-protein-coupled receptor 40 (GPR40), also known as free fatty acid (FFA) receptor 1, belongs to class A G-

protein-coupled receptors (GPCRs) and has a high affinity for medium- and long-chain saturated or unsaturated free fatty acid. GPR40 is located in various diverse organs such as the brain, pancreas, spinal cord, and heart [14–18]. Several studies have shown that the activation of GPR40 has had beneficial anti-inflammatory effects and provided neuro-protection after CNS injury [19–21]. Recent studies have shown that Eicosapentaenoic acid (EPA) elicits anti-inflammatory actions through the upregulation of GPR40 after acute cerebral infarction [22]. The activation of GPR40 potentiated the phosphorylation of p21-activated kinases4 (PAK4) in mouse islet cells [23]. Moreover, phosphorylated PAK4 has been shown to mediate the phosphorylation of CAMP-response element-binding (CREB), which promoted the protection of dopaminergic neurons in a rat model of PD and preserved motor function [24]. Recent studies also revealed that CREB induces the gene expression of histone H3 lysine 27 (H3K27) demethylase (KDM6B), which plays a role in the regulation of inflammatory gene expression and regulates phenotype switching of microglia from the M1 to M2 state [25–27]. Additionally, inhibition of KDM6B resulted in the attenuation of M2 microglia population, exacerbated the inflammatory response, and promoted M1 microglia [28, 29]. However, GPR40's role and its mechanism of action after GMH remain to be elucidated.

In this study, we demonstrated that GPR40 agonism attenuated pro-inflammatory cytokines, through the promotion M2-like microglia which improved short- and long-term neurological deficits in neonatal rat models of GMH through the PAK4/CREB/KDM6B signaling pathway.

Materials and methods

Animals

All experiments were approved by the Institutional Animal Care and Use Committee at Loma Linda University

and in compliance with the NIH Guidelines for the use of animals in neuroscience research. Two hundred and thirty-five P7 Sprague-Dawley neonatal pups (weight = 12–14 g, Harlan, Livermore, CA) were used.

Germinal matrix hemorrhage (GMH) model

The GMH model was induced by bacterial collagenase fusion as previously described in (Zhang et al., 2018) [30]. P7 neonatal pups were anesthetized using isoflurane (4% induction, 2% maintenance) and secured onto a neonatal stereotaxic frame. The skin along the longitudinal plane was incised exposing the bregma, which was followed by the drilling of a 1-mm burr hole into the skull at the following coordinates relative to bregma: 1.6 mm anterior and 1.5 mm right lateral. A 27-gauge needle with 0.3 U clostridial collagenase (Sigma-Aldrich, MO) was inserted at a depth of 2.7 mm from the dura through the burr hole and infused (1 μ l/min) using a 10 μ l Hamilton syringe (Hamilton Co., Reno, NV, USA) which was guided by a micro-infusion pump (Harvard Apparatus, Holliston, MA). The syringe was kept in place for an additional 5 min to avoid backflow. Lastly, the syringe was withdrawn at a speed of 0.5 mm/min, bone wax was used to close the burr hole, and the incision line was sutured. The animals were then placed onto a 37°C heated blanket for recovery and then reunited with the dam. Sham animals were operated on with needle insertion without collagenase infusion.

Experimental design

The current study was performed in four separate experiments.

Experiment 1: Time course of GPR40, p-PAK4, PAK4, KDM6B, CD16, CD206, and cellular localization of GPR40, KDM6B in P7 rat pups

Forty-two P7 rat pups were randomly divided into seven groups (n = 6 per group): Sham and GMH (3 h, 6 h, 12 h, 24 h, 3 days, 7 days). The whole brains of six rats from each group were collected for western blotting to determine the protein levels of GPR40, p-PAK4, PAK4, KDM6B, CD16, and CD206. The double immunofluorescence staining of GPR40 or KDM6B were used in the sham group and GMH (24 h) group (n = 3 per group) to evaluate the cellular localization of GPR40 or KDM6B in microglia, neurons, and astrocytes.

Experiment 2: The effects of GPR40 activation on short-term outcomes after GMH

Thirty P7 neonatal rat pups were randomly assigned to five groups (n = 6 per group): Sham; GMH + vehicle (10% dimethyl sulfide), GMH + GW9508 (0.84 mg/kg), GMH + GW9508 (2.5 mg/kg), and GMH + GW9508 (7.5 mg/kg). GW9508 was administrated intranasally (i.n.) 1

h, 25 h and 49 h after GMH. Neurological behavior tests were measured at 24 h, 48 h, and 72 h after GMH. Randomly, fifteen more rat pups were divided into three experimental groups with n = 5 for each group: Sham, GMH + vehicle (10% dimethyl sulfide), and GMH + GW9508 (best dose). These three groups were evaluated for microglia polarization by double immunofluorescence staining. The best dose of GW9508 was chosen based on the short-term neurological outcomes for the long-term outcome and mechanism experiments.

Experiment 3: The effect of GPR40 on long-term outcomes after GMH.

Sixty animals were randomly subjected to four groups (n = 15 per group): Sham, GMH + vehicle (10% dimethyl sulfide), GMH + GW9508, and GMH + GW9508 + GW1100 for evaluation of long-term neurological scores and histological result. GW9508 was administrated intranasally (i.n.) 1 h, 25 h, and 49 h after GMH. GW1100 was administrated intranasally (i.n.) 1 h before, and 23 h, 47 h after GMH. The rotarod and foot fault tests were performed on day 21 post-GMH. Morris water maze test was carried out on days 22–27 following GMH. Brain tissues were then obtained for Nissl staining to evaluate morphological changes.

Experiment 4: Mechanism study (GPR40/PAK4/CREB/KDM6B signaling pathway)

To investigate the potential molecular mechanism of GPR40 activation, 42 rats were randomly divided to seven groups (n = 6 per group): Sham, GMH + vehicle (10% dimethyl sulfide, i.n.), GMH + GW9508, GMH + GW9508 + scrambled CRISPR, GMH + GW9508 + GPR40 K.O. CRISPR, GMH + GW9508 + PAK4 K.O. CRISPR, GMH + GW9508 + KDM6B K.O. CRISPR. Furthermore, to determine the CRISPR/Cas9 editing efficiency, another 40 rats (n = 5 for each group) were randomly allocated into eight groups: naive + Scrambled CRISPR, naive + GPR40 K.O. CRISPR, naive + PAK4 K.O. CRISPR, naive + KDM6B K.O. CRISPR, GMH + scrambled CRISPR, GMH + GPR40 K.O. CRISPR, GMH + PAK4 K.O. CRISPR, GMH + KDM6B K.O. CRISPR. The whole brain was used for WB detection after neurological test.

Drug administration

Intranasal drug administration

Intranasal drug administration was conducted at 1 h, 25 h, and 49 h after GMH induction as described in (Zhang et al., 2017) [31]. A volume of 10 μ l was administered of either 10% dimethyl sulfide (vehicle) or GW9508 (G9797, Sigma Aldrich, MO) at three different dosages (0.84 mg/kg, 2.5 mg/kg, 7.5 mg/kg). The dosage of GW9508 was adapted from previous literature [32].

Intracerebroventricular drug administration

Intracerebroventricular (ICV) drug administration was delivered as previously described in (Flores et al., 2016) [3]. Briefly, the site of i.c.v injection was at the following coordinates relative to bregma: 1.0 mm posterior and 1.0 mm lateral. A 10 μ L Hamilton syringe (Microliter 701, Hamilton Company, Reno, NV, USA) was inserted through the burr hole into the left lateral ventricle at a depth of 1.8 mm. GPR40 CRISPR (Santa Cruz Biotechnology, Dallas, TX, USA), PAK4 CRISPR (Santa Cruz Biotechnology, Dallas, TX, USA), KDM6B CRISPR (Santa Cruz Biotechnology, Dallas, TX, USA), or Scramble CRISPR (Santa Cruz Biotechnology, Dallas, TX, USA) was infused into the ipsilateral ventricle 48 h prior to GMH induction. The needle was kept in place for 5 min and was slowly withdrawn over 3 min to prevent backflow.

Neurological performance

Short-term neurobehavioral examination

Negative geotaxis and right reflex were performed at 24 h, 48 h, and 72 h post-GMH as previously reported in (Feng et al., 2019) [33]. Negative geotaxis was conducted 3 times per pup, and the average time was obtained. Righting reflex was performed 3 times per rat pup, and the tests' average time was obtained. These two examinations were employed to evaluate the neurological function in neonate rat pups.

Long-term neurobehavioral examination

1. Rotarod test

Twenty-eight days post-ictus, rotarod test was conducted to assess the motor impairment as previously described in (Keleb et al., 2017) [34]. The duration of animals on the accelerating rotarod was recorded.

2. Foot fault test

Foot fault test was employed to assess changes in locomotor function [35]. The numbers of foot faults were recorded for 60s for each rat using a video recording device.

3. Morris water maze

The Morris water maze was used to evaluate spatial learning and memory at days 23–27 after GMH [36]. The water maze is made up of a plastic tub with an adjustable stand used as an escape for rats. Briefly, the rats were first trained to find the platform (cued test), which was then followed by the submerging of the platform (special test) where the rats would search for the

platform in a duration of 60 s. On the last day, the platform was removed and the rats were tested for memory reference (probe trial) for a duration of 60 s.

Immunofluorescence

Immunofluorescence was conducted as previously reported in (Pan et al., 2014, Pan et al., 2015) [37, 38]. Animals were anesthetized until unresponsive to stimuli, followed by trans-cardiac perfusion with ice-cold PBS. After the brains were removed, they were fixed in 10% formalin overnight at 4°C, then transferred to 30% sucrose until they sunk to the bottom. The brains were embedded and frozen at -80°C . Samples were segmented into 10 μm coronal slices. Next, the brain slices were incubated at 4°C overnight with primary antibodies: rabbit anti-GPR40 (1:50, PA5-75351, Thermo Fisher Scientific, MA, USA), rabbit anti-KDM6B (1:50, PA5-72751, Thermo Fisher Scientific, MA, USA), rabbit anti-CD11b (1:50, ab133357, Abcam, MA, USA), rabbit anti-CD206 (1:50, sc-58986, Santa Cruz Biotechnology, CA, USA), rabbit anti-CD16 (1:50, sc-58962, Santa Cruz Biotechnology, CA, USA), anti-NeuN (1:100, ab177487, Abcam, MA, USA), anti-Iba1 (1:100, ab15690, Abcam, MA, USA), and anti-GFAP (1:100, ab7260, Abcam, MA, USA). The brain slides were incubated with their respective secondary antibodies for 2 h at room temperature in a low-lit room. The cellular colocalization of GPR40 or KDM6B with NeuN, GFAP, and Iba1 was observed with the use of a fluorescence microscope (Leica DMi8, Buffalo Grove, IL). To observe microglia polarized populations, double immunofluorescence of CD16 or CD206 with CD11b was observed using the same fluorescence microscope.

Western blot

Western blot was conducted as previously reported [39–43]. The animal's whole brain tissue was obtained and extracted into RIPA lysis buffer (sc-24948, Santa Cruz Biotechnology, CA, USA), homogenized, and then centrifuged at 14,000 rpm at for 30 min. The equal amount of protein samples were loaded into 10% SDS-PAGE gel, then transferred to 0.22 μm nitrocellulose membranes, which were then incubated with the following primary antibodies: anti-GPR40 (1:1000, PA5-75351, Thermo Fisher Scientific, MA, USA), anti-PAK4 (1:500, sc-393367, Santa Cruz Biotechnology, CA, USA), anti-p-PAK4 (1:1000, PA5-64495, Thermo Fisher Scientific, MA, USA), anti-KDM6B (1:1000, PA5-72751, Thermo Fisher Scientific, MA, USA), anti-CREB (1:1000, 9197S Cell Signaling Technology Inc., MA, USA), anti-p-CREB (1:1000, 9198S Cell Signaling Technology Inc., MA, USA), anti-IL-1 β (1:1000, 12424S Cell Signaling Technology Inc., MA, USA), anti-TNF- α (1:1000, ab6671, Abcam, MA, USA), anti-CD206 (1:1000, sc-58986, Santa

Cruz Biotechnology, CA, USA), anti-IL-10 (1:1000, sc-365858, Santa Cruz Biotechnology, CA, USA), and anti- β -actin (1:3000, sc-47778, Santa Cruz Biotechnology, TX, USA) at 4 °C overnight. The membranes were then incubated with their respective secondary antibody (1:3000, Santa Cruz Biotechnology, Dallas, TX, USA and 1:5000, Millipore Sigma, Temecula, CA, USA) at room temperature for 1 h. For the quantification of western blot results, proteins and β -actin from the same sample and the same membrane corresponding to the proteins were detected. The results were normalized to the corresponding β -actin control.

Histological volumetric study

At 28 days post-ictus, the rats were euthanized and whole brains were extracted. Nissl staining was conducted and analyzed as previously reported in [44]. Sixteen-*micrometer*-thick brain sections were stained with 0.5% cresyl violet (Sigma-Aldrich), and the volume of ventricular and cortical thickness was calculated using ImageJ (ImageJ 1.52, NIH, USA). The volume was calculated with the following formula: average (area of coronal section) \times section interval \times number of sections as described in (Flores et al., 2016) [3].

Statistical analysis

All data are shown as the mean \pm SD. GraphPad Prism (Graph Pad Software, San Diego, CA, USA) was applied to analyze the data as previously described in (Pan et al., 2020) [45]. One-way analysis of variance ANOVA with Tukey's post hoc test was performed for comparison between multiple groups. Two-way analysis of variance ANOVA was performed to analyze the long-term neurobehavioral examinations. $p < 0.05$ was considered to be statistically significant.

Results

Endogenous GPR40, p-PAK4, and KDM6B were downregulated after GMH: GMH promptly increased CD16 expression, while endogenous CD206 expression was delayed until after 24 h

A time-course study was conducted to measure the endogenous expression levels of GPR40, p-PAK4, PAK4, and KDM6B after GMH via western blot. The expression of endogenous GPR40 decreased at 3 h and reached its lowest level at 24 h after GMH (Fig. 1a, b). However, the protein expression gradually increased at 3 and 7 days after GMH. Furthermore, the expressions of p-PAK4 and KDM6B demonstrated a similar downward trend in expression as GPR40 (Fig. 1a, c, and d).

Furthermore, double immunofluorescence staining of GPR40 or KDM6B with Iba-1 (microglia marker), GFAP (astrocytes), or NeuN (neurons) indicated that GPR40 and KDM6B were expressed in microglia (Figs. 2a, b and

3a, b), neurons (Figs. 2c and 3c), and astrocytes (Figs. 2d and 3d) in the neonatal rat CNS. The expression of GPR40-positive microglia and KDM6B-positive microglia were greater at 24 h after GMH when compared to the Sham group.

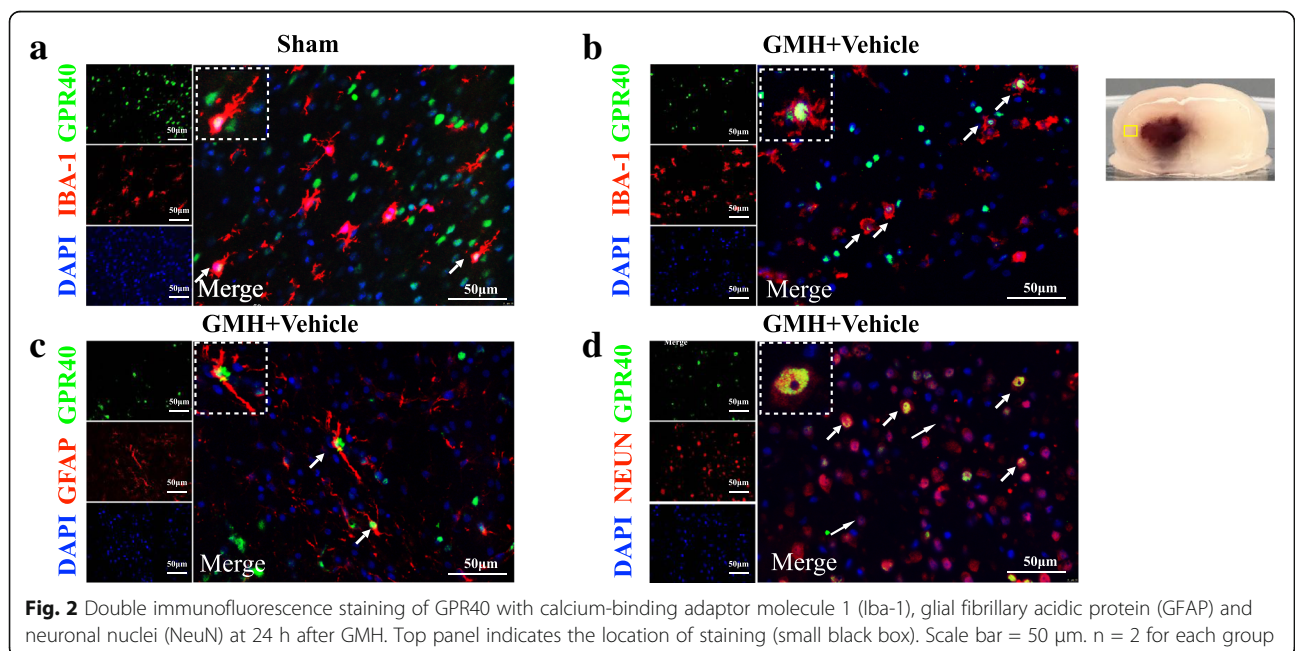
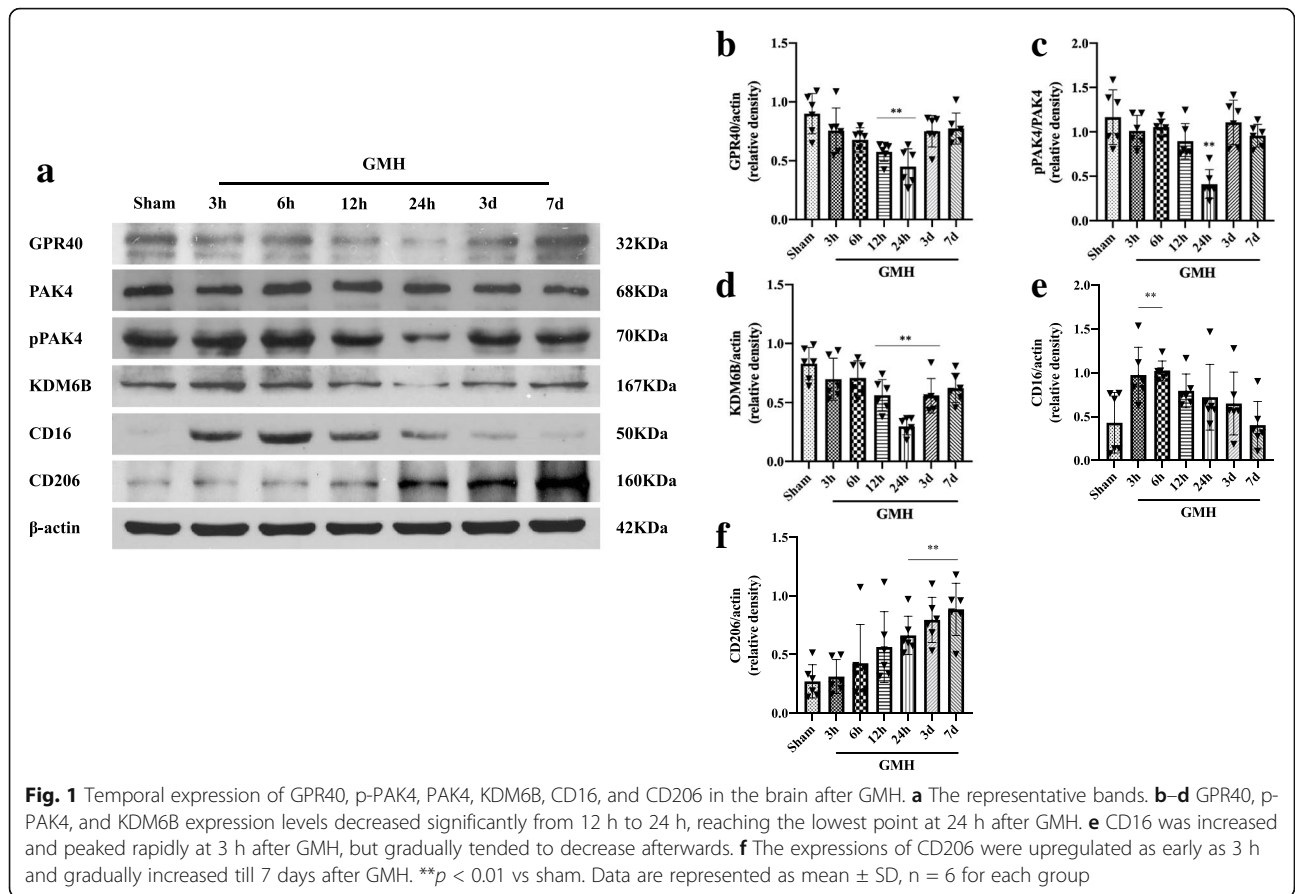
Endogenous CD16 expression initially peaked at 3 h after GMH (Fig. 1a, e). However, the protein expression gradually decreased at 12 h after GMH induction. Furthermore, the expressions of CD206 gradually increased for 7 consecutive days after GMH (Fig. 1a, f). M1 marker CD16 and M2 marker CD206 show inverse trends of expression.

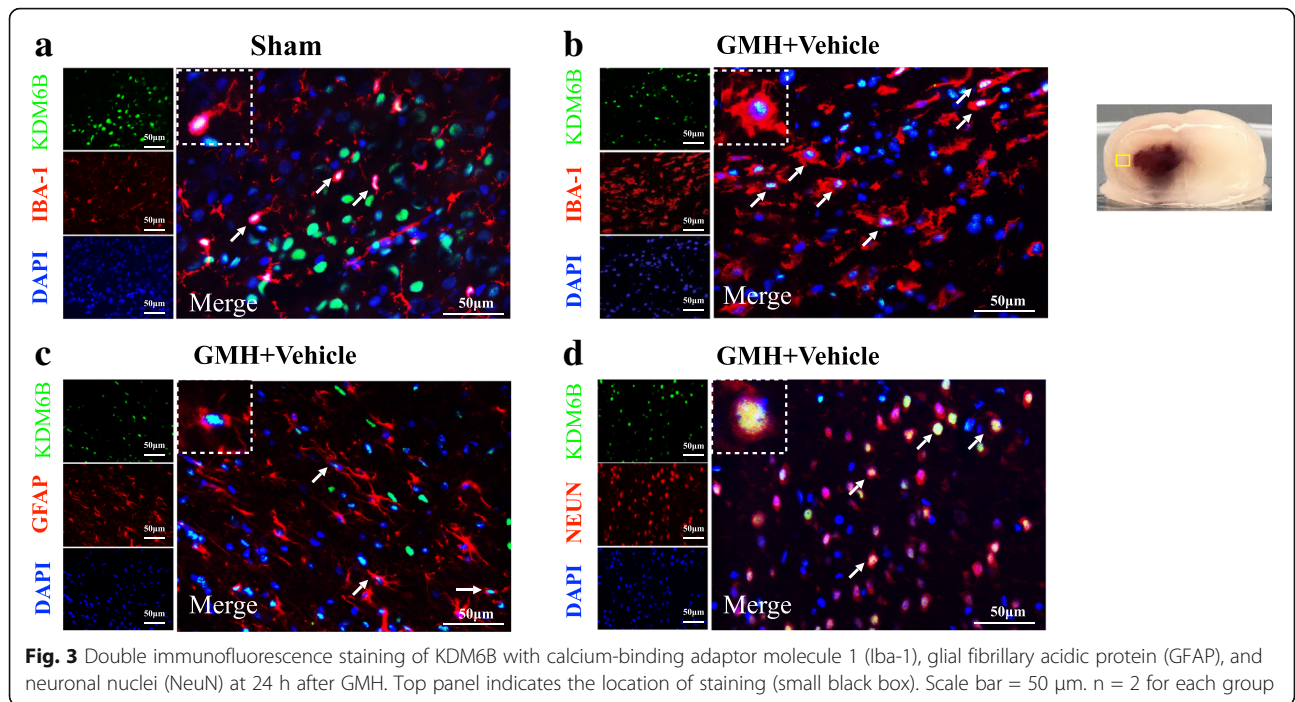
Intranasal administration of GW9508 improved short-term neurobehavioral outcomes at 3 days after GMH

Both short-term behavior test (negative geotaxis and right reflex test) demonstrated significant neurobehavioral deficits in the GMH + vehicle group in the first 3 days after GMH induction when compared to the Sham group (Fig. 4a–c). GW9508 treatment at a dosage of 2.5 mg/kg and 7.5 mg/kg demonstrated significant improvements in outcomes in the negative geotaxis 90-degree test when compared with the GMH + vehicle group in the first 3 days post-GMH (Fig. 4a). Additionally, GW9508 treatment at a dosage of 2.5 mg/kg demonstrated significant improvements on the negative geotaxis 180-degree test and the right reflex test compared with the GMH + vehicle group in the first 3 days post-GMH (Fig. 4b, c). In accordance with our results, the dosage of 2.5 mg/kg was chosen as the best dosage of GW9508 and will be used to investigate the effects of GPR40 activation in the long-term and signaling pathway.

GW9508 administration promoted proliferation of M2 microglia and inhibited M1 microglia in the periventricular area after GMH

Double immunofluorescence was used to detect M1 and M2 microglia populations. M1 microglia were quantified by the number of CD16- and CD11b-positive cells in the following three groups: sham, GMH + vehicle, and GMH + GW9508 treatment groups. The result demonstrated that the number of M1 microglia was significantly increased in GMH + vehicle group when compared to the sham group at 24 h after GMH (Fig. 5a, b, and d). However, the number of M1 microglia was decreased in the GMH + GW9508 treatment group when compared to the GMH + vehicle group at 24 h after GMH (Fig. 5c, d). The number of M2 microglia (CD206⁺/CD11b⁺ cells) in the GMH + vehicle group was significantly increased when compared with the sham group at 24 h after GMH (Fig. 6a, b, and d). Meanwhile, the number of M2 microglia significantly increased in the GMH+GW9508 treatment group





compared to both the GMH + vehicle and sham group at 24 h after GMH (Fig. 6c, d). The results suggested that GW9508 treatment reduced M1 microglia populations and increased M2 microglia populations at 24 h after GMH.

GW9508 treatment ameliorated long-term neurobehavioral impairment after GMH

Rotarod and foot fault tests were used to assess motor coordination. The GMH + vehicle group demonstrated

shorter falling latency in both 5 rpm and 10 rpm accelerating velocity experiments compared to the sham group at 28 days after GMH (Fig. 7a). GW9508 treatment improved the falling latency of GMH animals when compared to the GMH + vehicle group (Fig. 7a). However, the improvements induced by GW9508 treatment were reversed by GW1100 (a selective GPR40 antagonist) (Fig. 7a). The foot fault test demonstrated that rats in the vehicle group had a higher number of total foot

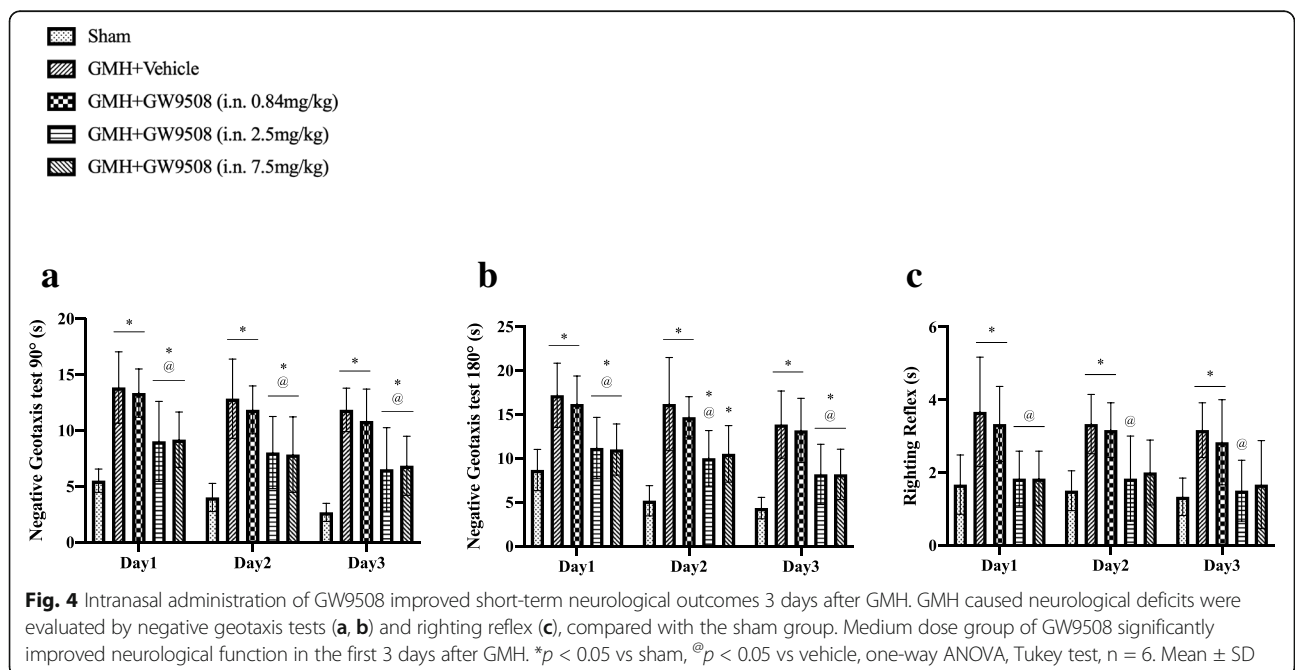
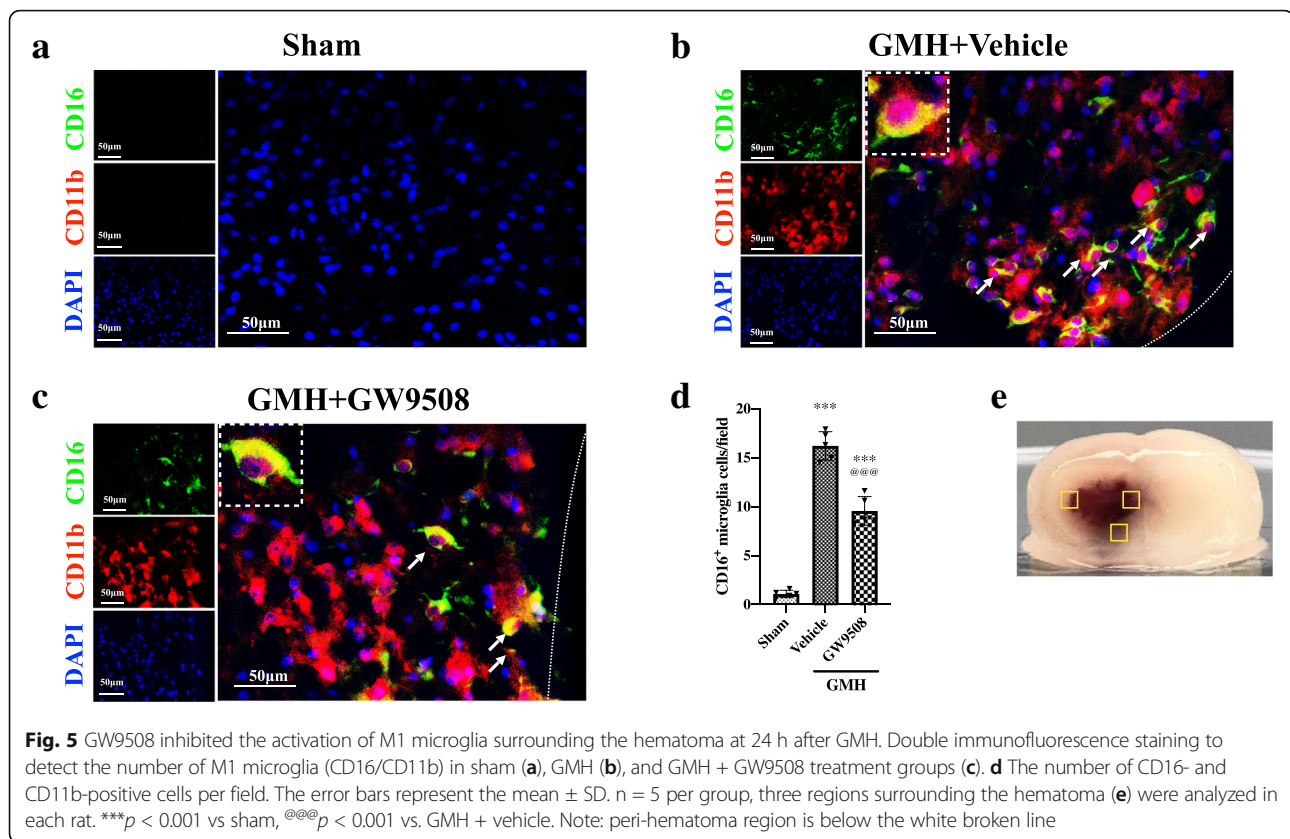


Fig. 4 Intranasal administration of GW9508 improved short-term neurological outcomes 3 days after GMH. GMH caused neurological deficits were evaluated by negative geotaxis tests (a, b) and righting reflex (c), compared with the sham group. Medium dose group of GW9508 significantly improved neurological function in the first 3 days after GMH. **p* < 0.05 vs sham, @*p* < 0.05 vs vehicle, one-way ANOVA, Tukey test, *n* = 6. Mean ± SD



faults when compared with the GW9508 treatment group (Fig. 7b). The effects of the treatment were reversed by GW1100 (Fig. 7b).

The Morris water maze was used to test spatial and reference memory after GMH. The water maze test demonstrated that vehicle animals had prolonged escape latency and increased swim distance (Fig. 8a, b) and spent significantly less time in the target quadrant in the probe trial (Fig. 8c) when compared with the sham group at 23–27 days after GMH. GMH rats treated with GW9508 had significantly improved spatial memory and learning, which resulted in decreased escape latency, swimming distance, and increase in time spent in the probe quadrant when compared to the GMH+ vehicle group (Fig. 8a, b, c, and e). However, the beneficial impact of GW9508 was reversed by GW1100 (Fig. 8a, b, c, and e). No significant difference was seen in the average swim speed between all three groups (Fig. 8d).

GW9508 attenuated ventriculomegaly and brain atrophy at day 28 after GMH

Nissl staining was performed to assess ventricular dilation and brain atrophy at 28 days after GMH. Ventricular volume was significantly increased in the vehicle and GW9508 + GW1100 groups, which was significantly reduced in the GW9508 treatment group (Fig. 9a, b). The

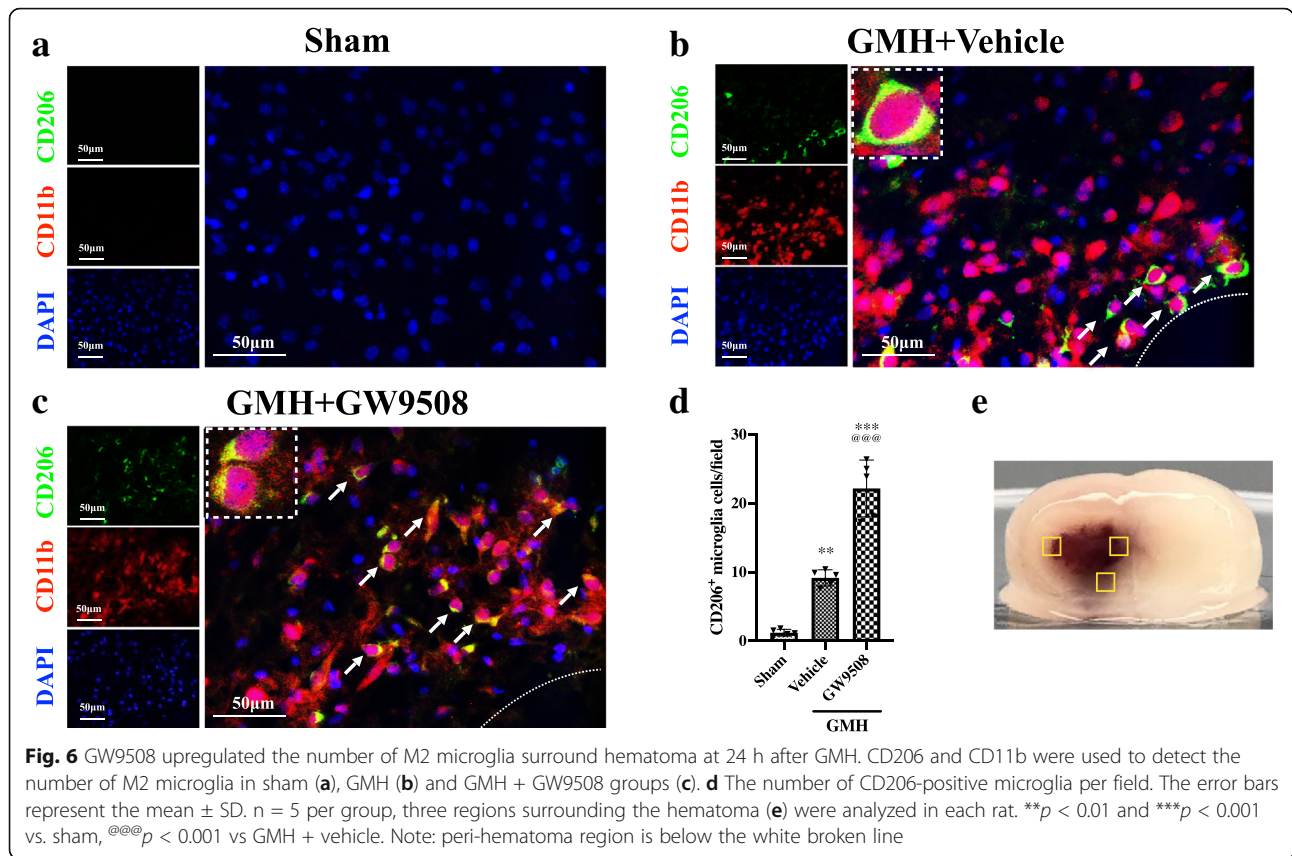
cortical thickness was significantly decreased in the vehicle and GW9508 + GW1100 group, whereas the GW9508 treatment significantly reduced cortical tissue loss (Fig. 9a, c).

GPR40 CRISPR, PAK4 CRISPR, and KDM6B CRISPR downregulated the expression of GPR40, PAK4, and KDM6B after GMH

Intraventricular injection of GPR40 K.O CRISPR, PAK4 K.O CRISPR, or KDM6B K.O CRISPR was given at 48 h prior GMH. CRISPRs significantly reduced the endogenous expression of GPR40, PAK4, or KDM6B in naive and GMH animals (Fig. 10). These results demonstrated the knockout efficacy of GPR40, PAK4, or KDM6B CRISPRs in the present study.

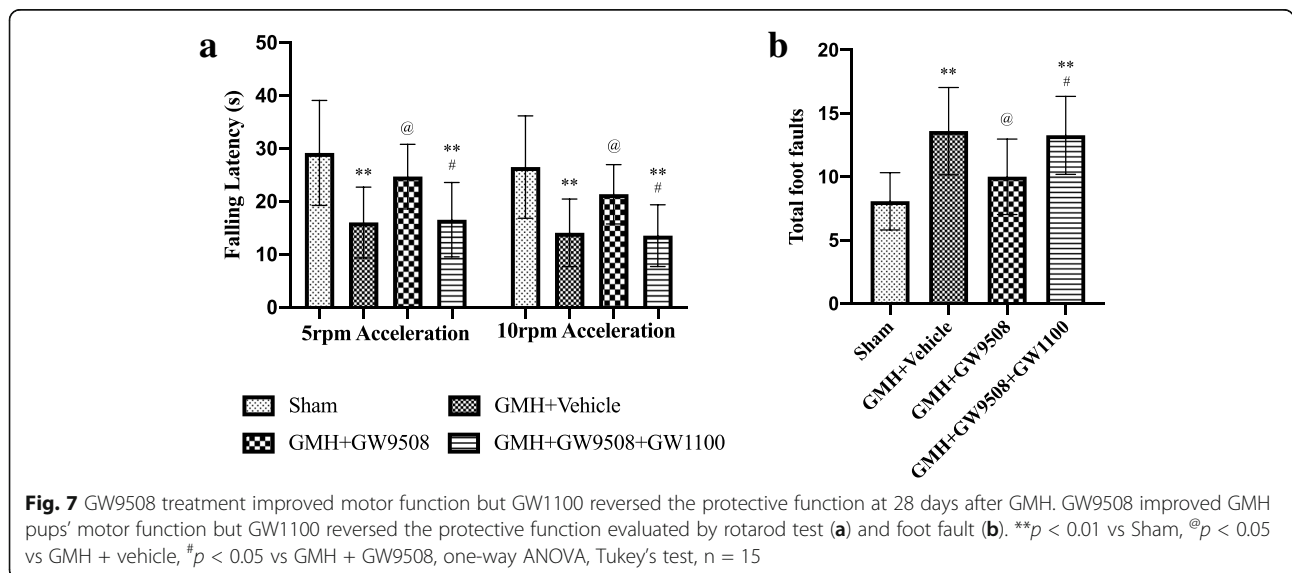
Activation of GPR40 via GW9508 attenuated inflammation and mediated microglia polarization via the PAK4/CREB/KDM6B signaling pathway at 24 h after GMH

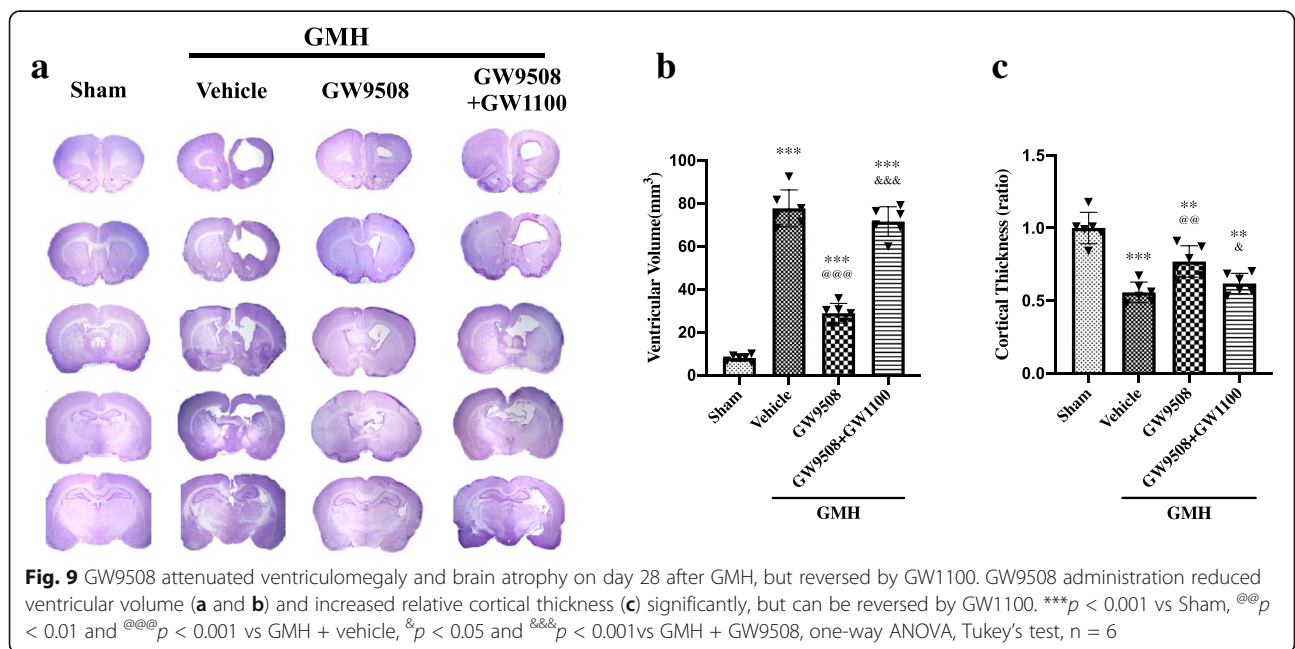
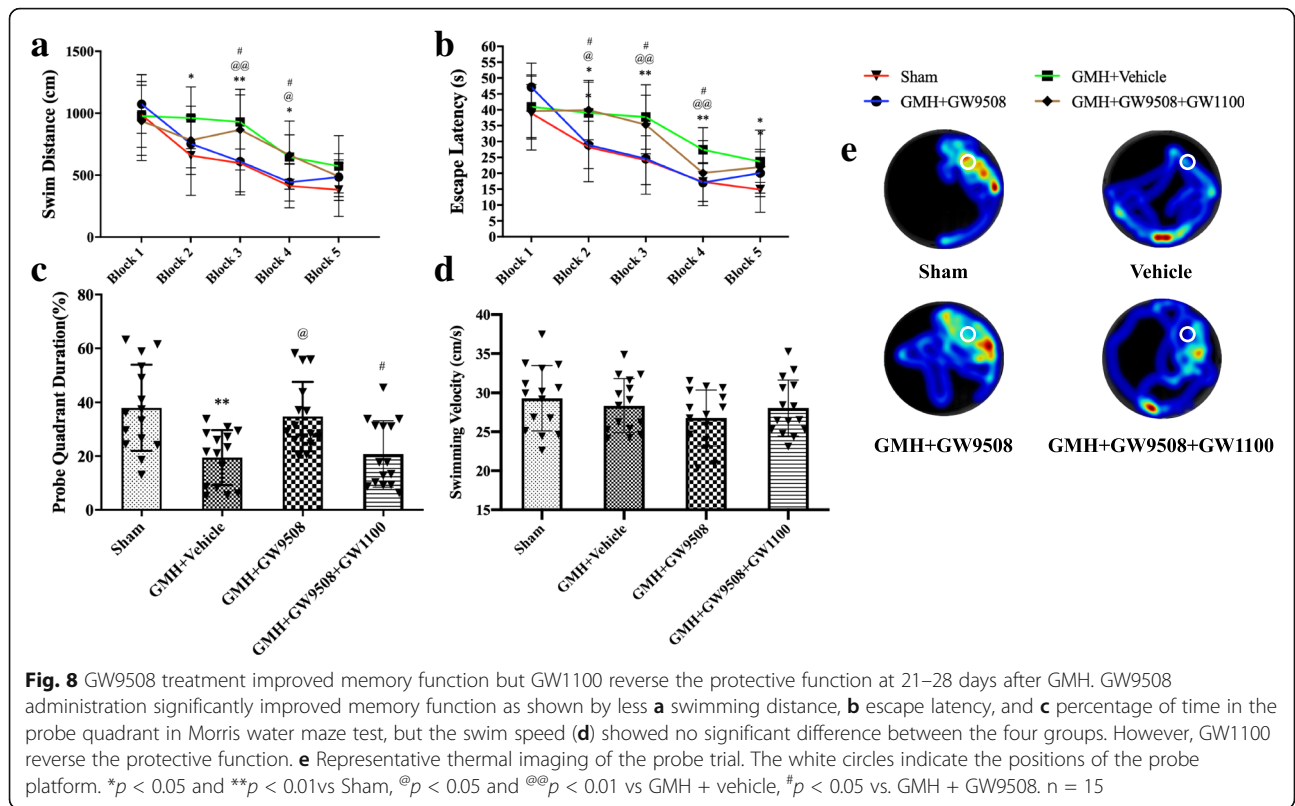
Western blots demonstrated that GMH significantly decreased the expression of GPR40, p-PAK4, p-CREB, and KDM6B, whereas GMH increased the level of IL-1 β , TNF- α , CD206, and IL-10 when compared with the sham group (Figs. 11 and 12). The activation of GPR40 by GW9508 treatment significantly increased the expression of p-PAK4, p-CREB, KDM6B, CD206, and IL-10,

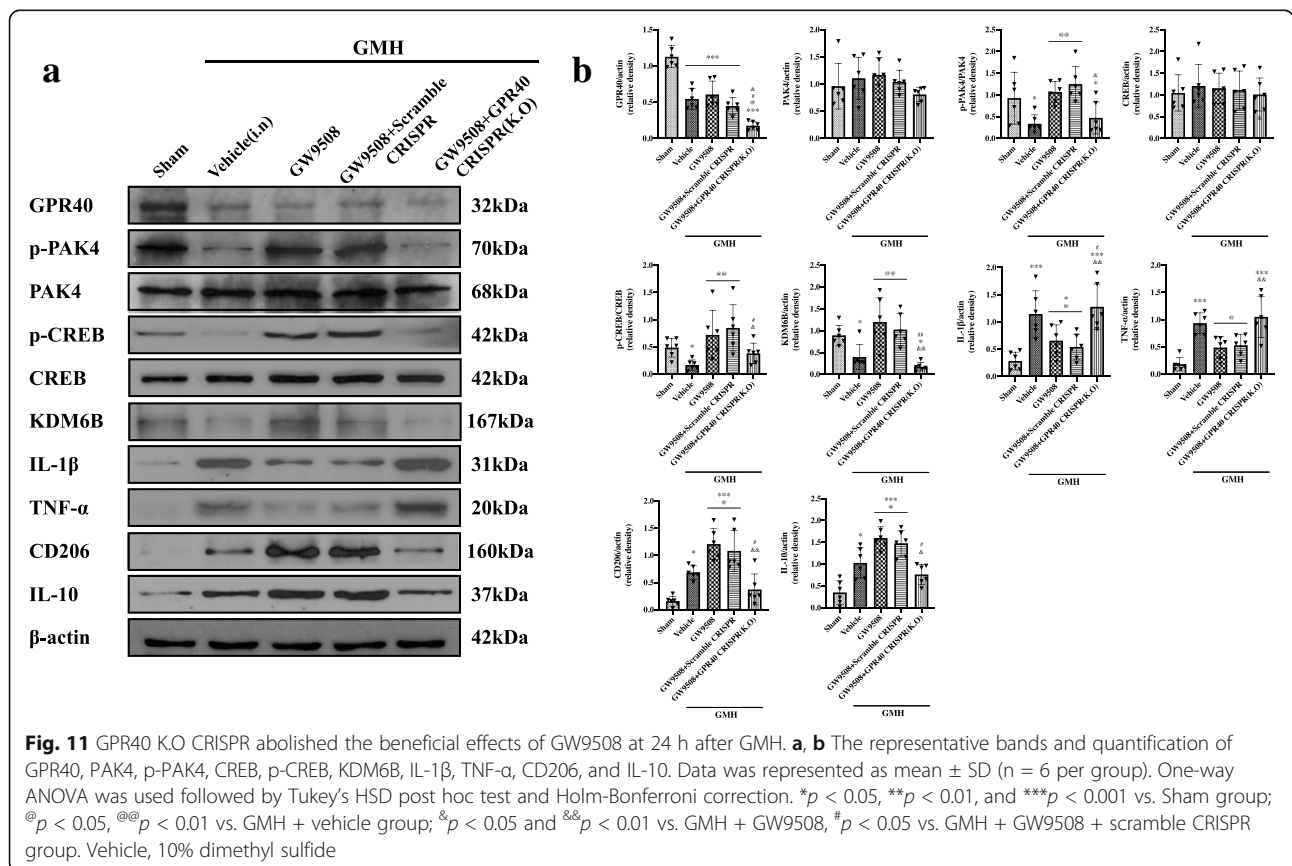
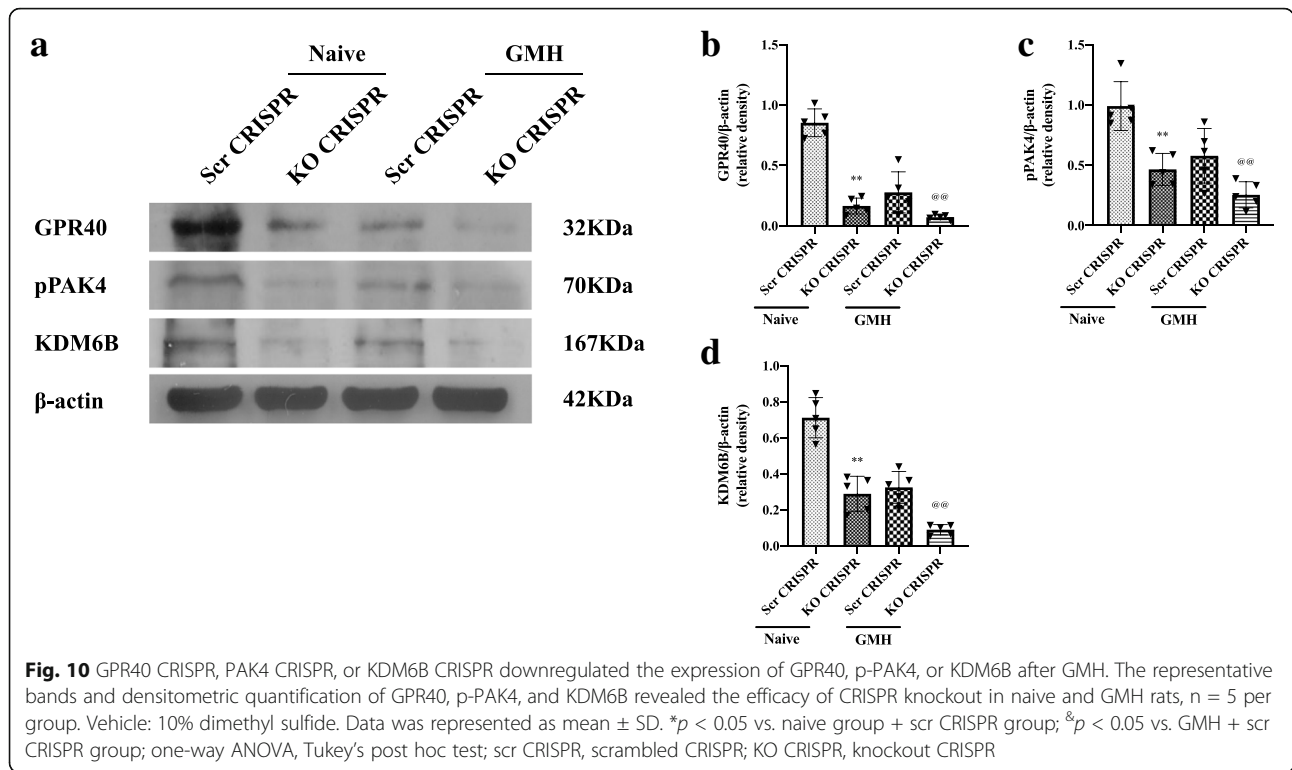


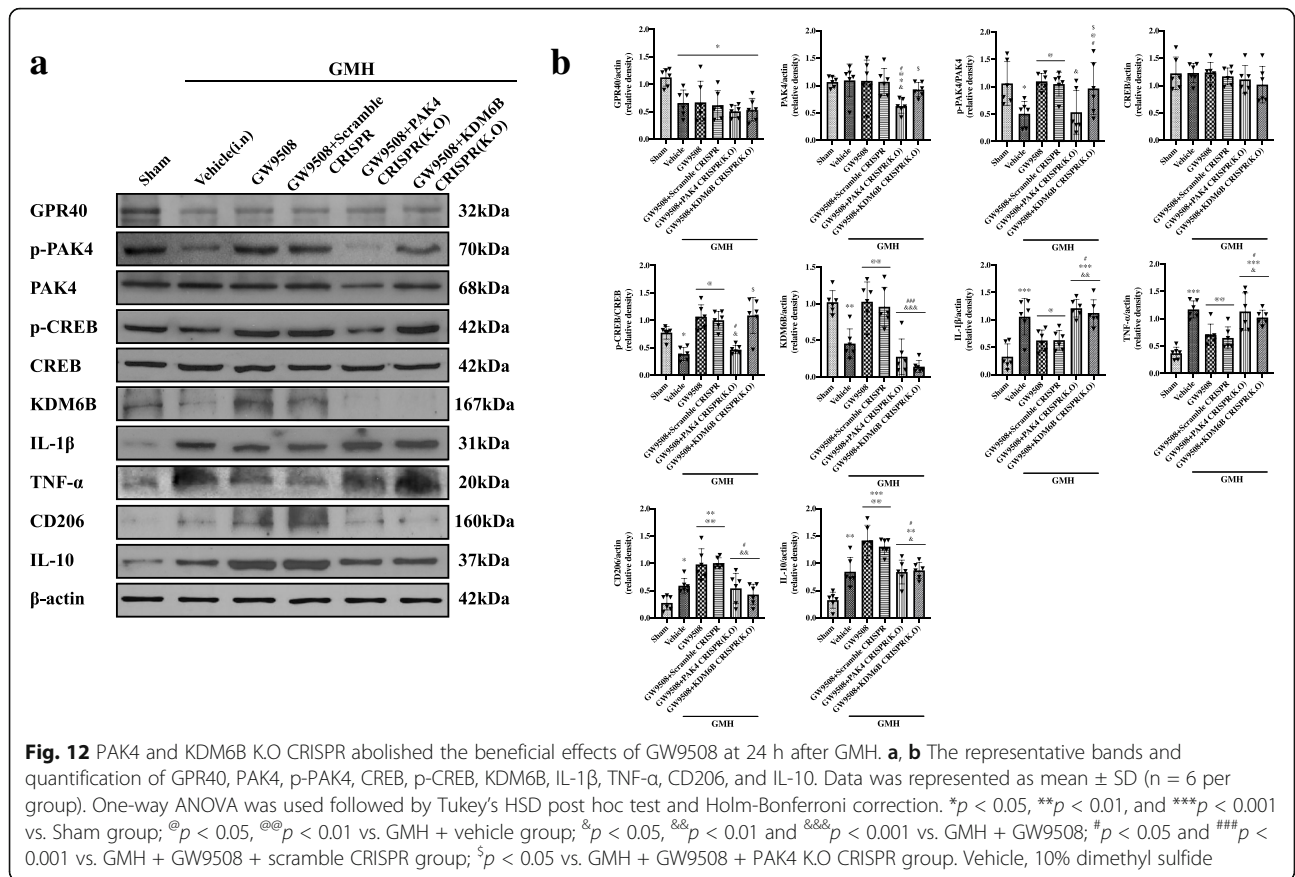
which was also met with a decrease in IL-1 β and TNF- α expression when compared to the GMH + vehicle group (Figs. 11 and 12). GPR40 K.O CRISPR significantly decreased the expression of GPR40, p-PAK4, p-CREB, KDM6B, CD206, and IL-10 and increased the expression of IL-1 β and TNF- α when compared to the GMH + GW9508 group and GMH + GW9508 + scramble CRIS

PR group (Fig. 11a, b). PAK4 K.O CRISPR significantly decreased the expression of p-PAK4, p-CREB, KDM6B, CD206, and IL-10 and significantly increased the protein level of IL-1 β and TNF- α compared to GMH + GW9508 group and GMH + GW9508 + scramble CRISPR group (Fig. 12a, b). Additionally, KDM6B K.O CRISPR significantly downregulated the protein level of KDM6B,









CD206, and IL-10 and increased the protein level of IL-1β and TNF-α compared to the GMH + GW9508 group and GMH + GW9508 + scramble CRISPR group (Fig. 12a, b). The results suggest that the PAK4/CREB/KDM6B signaling pathway plays a significant role in the attenuation of neuroinflammation and modifying microglia polarization through the activation of GPR40 after GMH.

Discussion

In this present study, we investigated the effect of GPR40 agonism via GW9508 on neuroinflammation and its underlying signaling mechanism after GMH. The novel findings of this study are as follows: (1) the expression of GPR40, p-PAK4, and KDM6B decreased at 3 h and reached the lowest level of expression at 24 h after GMH; the expression of M1 marker CD16 was significantly upregulated at 3 h after GMH, while M2 marker CD206 expression had a delayed increase in expression after GMH; (2) GPR40 and KDM6B were found to be expressed in neurons, astrocytes, and microglia at 24 h after GMH; (3) GW9508 at a dose of 2.5 mg/kg improved neurological outcomes at 24 h after GMH; (4) GW9508 attenuated neuroinflammation and decreased M1 and increased M2 microglia populations at 24 h

after GMH; (5) GW9508 improved long-term neurobehavior impairments and preserved brain morphology brought on by GMH; (6) and lastly, GPR40 agonism attenuated neuroinflammation and regulated microglia polarization via the PAK4/CREB/KDM6B signaling pathway.

GPR40, also known as free fatty acid receptor 1 (FFAR1), has been shown to be highly expressed in microglia, astrocytes, and neurons in the CNS [17]. Activation of GPR40 has been shown to attenuate the production of critical cytokines and chemokines [46]. The anti-inflammatory effects of GPR40 activation may be attributed to the inhibition of activated microglia (M1) populations through a GPR40-dependent manner. Current literature suggests that GPR40 agonisms play a role in the reduction in glial activation, which reduced subsequent neuronal damage in AD patients [47]. Additionally, intracerebroventricular treatment of GW9508, GPR40 agonist, reduced the expression of inflammatory genes in the hypothalamus and exerted neuroprotective effects after acute cerebral infarction [22, 48]. In the present study, we are the first to demonstrate that GMH decreased the expression of endogenous GPR40 in the neonatal CNS. Furthermore, double immunofluorescence staining showed that GPR40 was co-localized in

neurons, astrocytes, and microglia cells in the neonatal brain.

KDM6B (JMJD3) is one of two epigenetic modifiers responsible for the enzymatic removal of the repressive chromatin mark histone H3 lysine 27 trimethylation (H3K27me3). The demethylation of H3K27me3 is catalyzed by KDM6B which acts as a response gene to inflammatory cytokines and regulates macrophage polarization [49]. Suppression of KDM6B in microglia resulted in the decrease of M2 populations and was met with an exponential increase in M1 microglial populations, thereby increasing the inflammatory response which led to an extensive neuronal death [28]. An increase of microglial KDM6B expression was shown to attenuate inflammation and promoted anti-inflammatory effects of M2 after hemoglobin exposure, thereby suppressing inflammation in CNS injury models [27, 50]. In this present study, we are the first to demonstrate that GMH decreased the expression of endogenous KDM6B level in the brain. Meanwhile, double immunofluorescence staining showed that KDM6B was co-localized in neurons, astrocytes, and microglia cells.

Microglia are a unique cell type of immune/myeloid cells in the central nervous system [51]. Studies have shown that microglia are activated within minutes after CNS injury [52]. Current research indicates that microglia in the central nervous system are heterogeneous and can be widely present in polarized phenotypes [53]. The two phenotypes of interest are M1 microglia which mediate the production of inflammatory cytokines and alternatively activated M2 microglia which are characterized as anti-inflammatory modulators [54]. Our previous publications demonstrated that M2 microglia have been attributed to the improvement of both short- and long-term neurobehavioral outcomes after GMH [55]. Flores et al. demonstrated that the upregulation of CD36 in macrophages and microglia increased M2 microglia polarization and was critical for the enhancement of hematoma resolution, which improved overall outcomes [3]. Zhang et al. reported that rh-Chemerin attenuated GMH-induced neuroinflammation through M2 microglia polarization after GMH [30]. Our results demonstrated a significant increase in the number of CD206⁺ cells and decreased CD16⁺ cells in GW9508-treated GMH pups compared to the vehicle group. Our data suggest that the anti-inflammatory effects of GPR40 activation are attributed through microglia polarization.

We further explored the molecular mechanisms underlying the anti-inflammatory effects of GPR40 activation after GMH. The p21-activated kinases (PAKs) are a family of protein serine/threonine kinases [56]. Initial studies on PAK4 have revealed its role in the reorganization of the actin cytoskeleton, neuronal development, and regulation of axonal outgrowth in neural

progenitor cells. Previous studies indicated that the activation of the GPR40 enhanced PAK4 S474 phosphorylation [23]. CAMP-response element-binding (CREB) becomes activated by PAK4 phosphorylation, which in turn induces gene expression of KDM6B, which mediates inflammatory gene expression and regulates microglia polarization [24, 25]. In our present study, we demonstrated that the GPR40 activation by GW9508 significantly upregulated the expression of p-PAK4, p-CREB, KDM6B, CD206, and IL-10, but downregulated the protein levels of IL-1 β and TNF- α in the neonatal CNS at 24 h post-GMH. The knockdown of GPR40 decreased GPR40 expression and downstream signal molecules p-PAK4, p-CREB, KDM6B, CD206, and IL-10, while the knockdown resulted in the increased expression of IL-1 β and TNF- α . Furthermore, the knockdown of PAK4 significantly decreased the expression of p-PAK4, p-CREB, KDM6B, CD206, and IL-10, but increased the protein expression of IL-1 β and TNF- α . Lastly, the knockdown of KDM6B significantly reduced the protein level of KDM6B, CD206, and IL-10 and upregulated the protein level of IL-1 β and TNF- α . Our results indicate that GPR40 activation upregulates the KDM6B partly via the PAK4/CREB signaling pathway, demonstrating its role in anti-inflammation and microglia polarization after GMH.

The present study has several limitations. First, previous studies and our results revealed that GPR40 was also found to be localized in astrocytes and neurons. Yet this manuscript only focused on the mechanism of action of GPR40 in microglia cells, and further studies need to be conducted to establish the role of GPR40 on other cell types. Second, we verified a novel mechanism of the PAK4/CREB/KDM6B signaling pathway in the anti-inflammatory effect of GPR40 activation after GMH. However, other signaling pathways involved in the anti-inflammatory process such as AMPK/PLC/IP3 and TLR4/NF- κ B as well as ARRB2/NLRP3 need to be elucidated in future studies after GMH [57–59]. Third, although the collagenase injection model is a well-established and a consistent model to mimic the GMH pathophysiology, collagenase may exacerbate the inflammatory process and future studies need to be conducted to determine if collagenase significantly plays a role in the inflammatory process when modeling GMH [60]. Collagenase contribution to increased inflammation after GMH may account for the development of ventricular dilation. Therefore, it may differ from the cerebrovascular mechanism of a spontaneous cerebral hemorrhage in premature human newborns [61].

Conclusions

In conclusion, this study is the first to demonstrate that GPR40 agonism via GW9508 ameliorated neurobehavioral

impairments by attenuating neuroinflammation and regulating microglia polarization after GMH in neonatal rats. The anti-inflammatory and microglia polarization effects of GPR40 agonism were mediated, at least in part, through the PAK4/CREB/KDM6B signaling pathway. Therefore, GPR40 demonstrates promise in being a potential non-invasive target to attenuate neuroinflammation after GMH.

Abbreviations

BBB: Blood-brain barrier; BLVRA: Biliverdin reductase A; CNS: Central nervous system; CREB: CAMP-response element-binding; CRISPR: Clustered regularly interspaced short palindromic repeats; EPA: Eicosapentaenoic acid; FFA: Free fatty acid; FIZZ1: Hypoxia-induced mitogenic factor; GMH: Germinal matrix hemorrhage; GPR40: The orphan G-protein-coupled receptor 40; IL-10: Interleukin-10; IL-1 β : Interleukin-1 β ; IL-12: Interleukin-12; iNOS: Inducible nitric oxide synthase; KDM6B: Histone H3 lysine 27 (H3K27) demethylase; PAK4: p21-Activated kinases4; TNF- α : Tumor necrosis factor- α ; Ym1: Mouse chitinase 3-like 3

Acknowledgements

Not applicable.

Authors' contributions

JX participated in the research design, experimental performance (including animal surgery, Western blotting, and immunohistochemistry, but not the neurobehavioral testing), data analysis, and drafting of the manuscript. TC provided technical assistance and help with the manuscript preparation. RL discussed the results and edited parts of the manuscript. YL, WW, LG, QL, and LT performed the intracerebroventricular injection, co-immunoprecipitation, behavioral tests, and data analysis. JF and JHZ participated in the research design and edited the manuscript. HL and JT are the corresponding authors; these authors participated in all aspects of the study, including research design, data analysis, and manuscript preparation. The authors read and approved the final manuscript.

Funding

This study was supported in part by the NIH grant 5R21NS101284-02 by Dr. Jiping Tang.

Availability of data and materials

The datasets used and/or analyzed in the current study are available from the corresponding authors on request.

Declarations

Ethics approval and consent to participate

All animal experimental protocols were approved by the Loma Linda University Animal Care and Use Committees (IACUCs).

Consent for publication

Not applicable.

Competing interests

The authors declare that they have no competing interests.

Author details

¹Department of Emergency, The Third Xiangya Hospital of Central South University, 138 Tongzipo Road, Changsha, Hunan 410013, People's Republic of China. ²Department of Physiology and Pharmacology, Loma Linda University School of Medicine, Loma Linda, California 92354, USA.

³Department of Neurosurgery, The Third Xiangya Hospital of Central South University, 138 Tongzipo Road, Changsha, Hunan 410013, People's Republic of China. ⁴Departments of Anesthesiology, Neurosurgery and Neurology, Loma Linda University School of Medicine, Loma Linda, California 92354, USA. ⁵Center for Experimental Medicine, The Third Xiangya Hospital of Central South University, 138 Tongzipo Road, Changsha, Hunan 410013, People's Republic of China.

Received: 8 March 2021 Accepted: 1 July 2021

Published online: 18 July 2021

References

- Ding Y, Zhang T, Wu G, McBride DW, Xu N, Klebe DW, et al. Astroglial inhibition attenuates hydrocephalus by increasing cerebrospinal fluid reabsorption through the glymphatic system after germinal matrix hemorrhage. *Exp Neurol*. 2019;320:113003. <https://doi.org/10.1016/j.expneurol.2019.113003>.
- Tang J, Tao Y, Jiang B, Chen Q, Hua F, Zhang J, et al. Pharmacological preventions of brain injury following experimental germinal matrix hemorrhage: an up-to-date review. *Transl Stroke Res*. 2016;7(1):20–32. <https://doi.org/10.1007/s12975-015-0432-8>.
- Flores JJ, Klebe D, Rolland WB, Lekic T, Krafft PR, Zhang JH. PPAR γ -induced upregulation of CD36 enhances hematoma resolution and attenuates long-term neurological deficits after germinal matrix hemorrhage in neonatal rats. *Neurobiol Dis*. 2016; [cited 2020 Oct 21];87:124–33. Available from: <http://www.sciencedirect.com/science/article/pii/S0969996115301169>.
- Perry VH, Teeling J. Microglia and macrophages of the central nervous system: the contribution of microglia priming and systemic inflammation to chronic neurodegeneration. *Semin Immunopathol*. 2013; [cited 2020 Oct 21];35:601–12. Available from: <https://www.ncbi.nlm.nih.gov/pmc/articles/PMC3742955/>.
- van Dijk BJ, Meijers JCM, Kloek AT, Knaup VL, Rinkel GJE, Morgan BP, et al. Complement C5 contributes to brain injury after subarachnoid hemorrhage. *Transl Stroke Res*. 2020;11(4):678–88. <https://doi.org/10.1007/s12975-019-00757-0>.
- Tschoe C, Bushnell CD, Duncan PW, Alexander-Miller MA, Wolfe SQ. Neuroinflammation after intracerebral hemorrhage and potential therapeutic targets. *J Stroke*. 2020;22(1):29–46. <https://doi.org/10.5853/jos.2019.02236>.
- Colton CA. Heterogeneity of microglial activation in the innate immune response in the brain. *J Neuroimmune Pharmacol Off J Soc NeuroImmune Pharmacol*. 2009;4(4):399–418. <https://doi.org/10.1007/s11481-009-9164-4>.
- Fumagalli S, Perego C, Pischotta F, Zanier ER, De Simoni M-G. The ischemic environment drives microglia and macrophage function. *Front Neurol*. 2015; [cited 2021 Feb 8];6. Available from: <https://www.ncbi.nlm.nih.gov/pmc/articles/PMC4389404/>.
- Gomes-Leal W. Microglial physiopathology: how to explain the dual role of microglia after acute neural disorders? *Brain Behav*. 2012;2(3):345–56. <https://doi.org/10.1002/brb3.51>.
- Zhao X, Sun G, Zhang J, Strong R, Song W, Gonzales N, et al. Hematoma resolution as a target for intracerebral hemorrhage treatment: role for peroxisome proliferator-activated receptor gamma in microglia/macrophages. *Ann Neurol*. 2007;61(4):352–62. <https://doi.org/10.1002/ana.21097>.
- Cai Y, Xu T-T, Lu C-Q, Ma Y-Y, Chang D, Zhang Y, et al. Endogenous regulatory t cells promote M2 macrophage phenotype in diabetic stroke as visualized by optical imaging. *Transl Stroke Res*. 2020.
- Lee J-Y, Castelli V, Bonsack B, Coats AB, Navarro-Torres L, Garcia-Sanchez J, et al. A novel partial MHC class II construct, DRmQ, inhibits central and peripheral inflammatory responses to promote neuroprotection in experimental stroke. *Transl Stroke Res*. 2020;11(4):831–6. <https://doi.org/10.1007/s12975-019-00756-1>.
- Jackson L, Dong G, Althomali W, Sayed MA, Eldahshan W, Baban B, et al. Delayed administration of angiotensin II type 2 receptor (AT2R) agonist compound 21 prevents the development of post-stroke cognitive impairment in diabetes through the modulation of microglia polarization. *Transl Stroke Res*. 2020;11(4):762–75. <https://doi.org/10.1007/s12975-019-00752-5>.
- Furukawa H, Miyamoto Y, Hirata Y, Watanabe K, Hitomi Y, Yoshitomi Y, et al. Design and identification of a GPR40 full agonist (SCO-267) possessing a 2-carbamoylphenyl piperidine moiety. *J Med Chem*. 2020;63(18):10352–79. <https://doi.org/10.1021/acs.jmedchem.0c00843>.
- Briscoe CP, Tadayyon M, Andrews JL, Benson WG, Chambers JK, Eilert MM, et al. The orphan G protein-coupled receptor GPR40 is activated by medium and long chain fatty acids. *J Biol Chem*. 2003;278(13):11303–11. <https://doi.org/10.1074/jbc.M211495200>.
- Itoh Y, Kawamata Y, Harada M, Kobayashi M, Fujii R, Fukusumi S, et al. Free fatty acids regulate insulin secretion from pancreatic beta cells through GPR40. *Nature*. 2003;422(6928):173–6. <https://doi.org/10.1038/nature01478>.

17. Ma D, Tao B, Warashina S, Kotani S, Lu L, Kaplamadzhiev DB, et al. Expression of free fatty acid receptor GPR40 in the central nervous system of adult monkeys. *Neurosci Res.* 2007;58(4):394–401. <https://doi.org/10.1016/j.neures.2007.05.001>.
18. Ma D, Lu L, Boneva NB, Warashina S, Kaplamadzhiev DB, Mori Y, et al. Expression of free fatty acid receptor GPR40 in the neurogenic niche of adult monkey hippocampus. *Hippocampus.* 2008;18(3):326–33. <https://doi.org/10.1002/hipo.20393>.
19. Mao X-F, Wu H-Y, Tang X-Q, Ali U, Liu H, Wang Y-X. Activation of GPR40 produces mechanical allodynia via the spinal glial interleukin-10/ β -endorphin pathway. *J Neuroinflammation.* 2019 [cited 2020 Oct 22];16. Available from: <https://www.ncbi.nlm.nih.gov/pmc/articles/PMC6461825/>.
20. Ma D, Zhang M, Larsen CP, Xu F, Hua W, Yamashima T, et al. DHA promotes the neuronal differentiation of rat neural stem cells transfected with GPR40 gene. *Brain Res.* 2010;1330:1–8. <https://doi.org/10.1016/j.brainres.2010.03.002>.
21. Nakamoto K, Nishinaka T, Sato N, Mankura M, Koyama Y, Kasuya F, et al. Hypothalamic GPR40 signaling activated by free long chain fatty acids suppresses CFA-induced inflammatory chronic pain. *PLoS One.* 2013;8(12):e81563. <https://doi.org/10.1371/journal.pone.0081563>.
22. Mo Z, Tang C, Li H, Lei J, Zhu L, Kou L, et al. Eicosapentaenoic acid prevents inflammation induced by acute cerebral infarction through inhibition of NLRP3 inflammasome activation. *Life Sci.* 2020;242:117133. <https://doi.org/10.1016/j.lfs.2019.117133>.
23. Bergeron V, Ghislain J, Poutout V. The P21-activated kinase PAK4 is implicated in fatty-acid potentiation of insulin secretion downstream of free fatty acid receptor 1. *Islets.* 2016;8(6):157–64. <https://doi.org/10.1080/19382014.2016.1243191>.
24. Won S-Y, Park J-J, Shin E-Y, Kim E-G. PAK4 signaling in health and disease: defining the PAK4-CREB axis. *Exp Mol Med.* 2019;51(2):1–9. <https://doi.org/10.1038/s12276-018-0204-0>.
25. Alexaki VI, Fodelianaki G, Neuwirth A, Mund C, Kourgiantaki A, Ieronimaki E, et al. DHEA inhibits acute microglia-mediated inflammation through activation of the TrkA-Akt1/2-CREB-Jmjd3 pathway. *Mol Psychiatry.* 2018; 23(6):1410–20. <https://doi.org/10.1038/mp.2017.167>.
26. Przanowski P, Dabrowski M, Ellert-Miklaszewska A, Kloss M, Mieczkowski J, Kaza B, et al. The signal transducers Stat1 and Stat3 and their novel target Jmjd3 drive the expression of inflammatory genes in microglia. *J Mol Med Berl Ger.* 2014;92(3):239–54. <https://doi.org/10.1007/s00109-013-1090-5>.
27. Tao T, Liu G-J, Shi X, Zhou Y, Lu Y, Gao Y-Y, et al. DHEA attenuates microglial activation via induction of JMJD3 in experimental subarachnoid haemorrhage. *J Neuroinflammation.* 2019;16(1):243. <https://doi.org/10.1186/s12974-019-1641-y>.
28. Tang Y, Li T, Li J, Yang J, Liu H, Zhang XJ, et al. Jmjd3 is essential for the epigenetic modulation of microglia phenotypes in the immune pathogenesis of Parkinson's disease. *Cell Death Differ.* 2014;21(3):369–80. <https://doi.org/10.1038/cdd.2013.159>.
29. Satoh T, Takeuchi O, Vandenbon A, Yasuda K, Tanaka Y, Kumagai Y, et al. The Jmjd3-Irf4 axis regulates M2 macrophage polarization and host responses against helminth infection. *Nat Immunol.* 2010;11(10):936–44. <https://doi.org/10.1038/ni.1920>.
30. Zhang Y, Xu N, Ding Y, Zhang Y, Li Q, Flores J, et al. Chemerin suppresses neuroinflammation and improves neurological recovery via CaMKK2/AMPK/Nrf2 pathway after germinal matrix hemorrhage in neonatal rats. *Brain Behav Immun.* 2018;70:179–93. <https://doi.org/10.1016/j.bbi.2018.02.015>.
31. Zhang Y, Ding Y, Lu T, Zhang Y, Xu N, Yu L, et al. Bliverdin reductase-A improves neurological function in a germinal matrix hemorrhage rat model. *Neurobiol Dis.* 2018;110:122–32. <https://doi.org/10.1016/j.nbd.2017.11.017>.
32. Khan MZ, Zhuang X, He L. GPR40 receptor activation leads to CREB phosphorylation and improves cognitive performance in an Alzheimer's disease mouse model. *Neurobiol Learn Mem.* 2016;131:46–55. <https://doi.org/10.1016/j.nlm.2016.03.006>.
33. Feng Z, Ye L, Klebe D, Ding Y, Guo Z-N, Flores JJ, et al. Anti-inflammation conferred by stimulation of CD200R1 via Dok1 pathway in rat microglia after germinal matrix hemorrhage. *J Cereb Blood Flow Metab Off J Int Soc Cereb Blood Flow Metab.* 2019;39(1):97–107. <https://doi.org/10.1177/0271678X17725211>.
34. Klebe D, Flores JJ, McBride DW, Krafft PR, Rolland WB, Lelic T, et al. Dabigatran ameliorates post-haemorrhagic hydrocephalus development after germinal matrix haemorrhage in neonatal rat pups. *J Cereb Blood Flow Metab Off J Int Soc Cereb Blood Flow Metab.* 2017;37(9):3135–49. <https://doi.org/10.1177/0271678X16684355>.
35. Webb RL, Kaiser EE, Scoville SL, Thompson TA, Fatima S, Pandya C, et al. Human neural stem cell extracellular vesicles improve tissue and functional recovery in the murine thromboembolic stroke model. *Transl Stroke Res.* 2018;9(5):530–9. <https://doi.org/10.1007/s12975-017-0599-2>.
36. Ran H, Yuan J, Huang J, Wang J, Chen K, Zhou Z. Adenosine A2A receptors in bone marrow-derived cells attenuate cognitive impairment in mice after chronic hypoperfusion white matter injury. *Transl Stroke Res.* 2020;11(5):1028–40. <https://doi.org/10.1007/s12975-019-00778-9>.
37. Pan B, Yang L, Wang J, Wang Y, Wang J, Zhou X, et al. C-Abl tyrosine kinase mediates neurotoxic prion peptide-induced neuronal apoptosis via regulating mitochondrial homeostasis. *Mol Neurobiol.* 2014;49(2):1102–16. <https://doi.org/10.1007/s12035-014-8646-4>.
38. Pan Y, Sun L, Wang J, Fu W, Fu Y, Wang J, et al. STI571 protects neuronal cells from neurotoxic prion protein fragment-induced apoptosis. *Neuropharmacology.* 2015;93:191–8. <https://doi.org/10.1016/j.neuropharm.2015.01.029>.
39. Zheng X, Zhang L, Kuang Y, Venkataramani V, Jin F, Hein K, et al. Extracellular vesicles derived from neural progenitor cells—a preclinical evaluation for stroke treatment in mice. *Transl Stroke Res.* 2020.
40. Pan B, Zhang H, Cui T, Wang X. TFEB activation protects against cardiac proteotoxicity via increasing autophagic flux. *J Mol Cell Cardiol.* 2017;113:51–62. <https://doi.org/10.1016/j.yjmcc.2017.10.003>.
41. Pan B, Lewno MT, Wu P, Wang X. Highly dynamic changes in the activity and regulation of macroautophagy in hearts subjected to increased proteotoxic stress. *Front Physiol.* 2019;10:758. <https://doi.org/10.3389/fphys.2019.00758>.
42. Fang Y, Shi H, Ren R, Huang L, Okada T, Lenahan C, et al. Pituitary adenylate cyclase-activating polypeptide attenuates brain edema by protecting blood-brain barrier and glymphatic system after subarachnoid hemorrhage in rats. *Neurother J Am Soc Exp Neurother.* 2020;17:1954–72.
43. Luo Y, Fang Y, Kang R, Lenahan C, Gamdzik M, Zhang Z, et al. Inhibition of EZH2 (enhancer of zeste homolog 2) attenuates neuroinflammation via H3k27me3/SOCS3/TRAF6/NF- κ B (trimethylation of histone 3 lysine 27/ suppressor of cytokine signaling 3/tumor necrosis factor receptor family 6/ nuclear factor- κ B) in a rat model of subarachnoid hemorrhage. *Stroke.* 2020; 51(11):3320–31. <https://doi.org/10.1161/STROKEAHA.120.029951>.
44. Wang Z, Zhou F, Dou Y, Tian X, Liu C, Li H, et al. Melatonin alleviates intracerebral hemorrhage-induced secondary brain injury in rats via suppressing apoptosis, inflammation, oxidative stress, DNA damage, and mitochondria injury. *Transl Stroke Res.* 2018;9(1):74–91. <https://doi.org/10.1007/s12975-017-0559-x>.
45. Pan B, Li J, Parajuli N, Tian Z, Wu P, Lewno MT, et al. The calcineurin-TFEB-p62 pathway mediates the activation of cardiac macroautophagy by proteasomal malfunction. *Circ Res.* 2020;127(4):502–18. <https://doi.org/10.1161/CIRCRESAHA.119.316007>.
46. Fujita T, Matsuoka T, Honda T, Kabashima K, Hirata T, Narumiya S. A GPR40 agonist GW9508 suppresses CCL5, CCL17, and CXCL10 induction in keratinocytes and attenuates cutaneous immune inflammation. *J Invest Dermatol.* 2011;131(8):1660–7. <https://doi.org/10.1038/jid.2011.123>.
47. Nishimura Y, Moriyama M, Kawabe K, Satoh H, Takano K, Azuma Y-T, et al. Lauric acid alleviates neuroinflammatory responses by activated microglia: involvement of the GPR40-dependent pathway. *Neurochem Res.* 2018;43(9):1723–35. <https://doi.org/10.1007/s11064-018-2587-7>.
48. Dragano NR, Solon C, Ramalho AF, de Moura RF, Razolli DS, Christiansen E, et al. Polyunsaturated fatty acid receptors, GPR40 and GPR120, are expressed in the hypothalamus and control energy homeostasis and inflammation. *J Neuroinflammation.* 2017;14(1):91. <https://doi.org/10.1186/s12974-017-0869-7>.
49. De Santa F, Totaro MG, Prosperini E, Notarbartolo S, Testa G, Natoli G. The histone H3 lysine-27 demethylase Jmjd3 links inflammation to inhibition of polycomb-mediated gene silencing. *Cell.* 2007;130(6):1083–94. <https://doi.org/10.1016/j.cell.2007.08.019>.
50. Jin M, Li Q, Gu Y, Wan B, Huang J, Xu X, et al. Leonurine suppresses neuroinflammation through promoting oligodendrocyte maturation. *J Cell Mol Med.* 2019;23(2):1470–85. <https://doi.org/10.1111/jcmm.14053>.
51. Wang J, Zhao D, Pan B, Fu Y, Shi F, Kouadir M, et al. Toll-like receptor 2 deficiency shifts PrP106-126-induced microglial activation from a neurotoxic to a neuroprotective phenotype. *J Mol Neurosci.* 2015 [cited 2021 May 7]; 55:880–90. Available from: <https://doi.org/10.1007/s12031-014-0442-0>.
52. Taylor RA, Sansing LH. Microglial responses after ischemic stroke and intracerebral hemorrhage. *Clin Dev Immunol.* 2013; [cited 2020 Nov 11];2013. Available from: <https://www.ncbi.nlm.nih.gov/pmc/articles/PMC3810327/>.

53. Zhang L, Zhang J, You Z. Switching of the microglial activation phenotype is a possible treatment for depression disorder. *Front Cell Neurosci.* 2018; [cited 2020 Nov 11];12. Available from: <https://www.ncbi.nlm.nih.gov/pmc/articles/PMC6232769/>.
54. Cherry JD, Olschowka JA, O'Banion MK. Neuroinflammation and M2 microglia: the good, the bad, and the inflamed. *J Neuroinflammation.* 2014; [cited 2020 Nov 11];11:98. Available from: <https://www.ncbi.nlm.nih.gov/pmc/articles/PMC4060849/>.
55. Zhang Y, Ding Y, Lu T, Zhang Y, Xu N, Yu L, et al. Bliverdin reductase-a improves neurological function in a germinal matrix hemorrhage rat model. *Neurobiol Dis.* 2018; [cited 2020 Nov 11];110:122–32. Available from: <https://www.ncbi.nlm.nih.gov/pmc/articles/PMC5747982/>.
56. Qu J, Li X, Novitch BG, Zheng Y, Kohn M, Xie J-M, et al. PAK4 kinase is essential for embryonic viability and for proper neuronal development. *Mol Cell Biol.* 2003;23(20):7122–33. <https://doi.org/10.1128/MCB.23.20.7122-7133.2003>.
57. Shen X, Fan B, Hu X, Luo L, Yan Y, Yang L. Metformin reduces lipotoxicity-induced meta-inflammation in β -cells through the activation of GPR40-PLC-IP3 pathway. *J Diabetes Res.* 2019;2019:7602427.
58. Chen X, Yan Y, Weng Z, Chen C, Lv M, Lin Q, et al. TAK-875 mitigates β -cell lipotoxicity-induced metaflammation damage through inhibiting the TLR4-NF- κ B pathway. *J Diabetes Res.* 2019; [cited 2020 Nov 11]. Available from: <https://pubmed.ncbi.nlm.nih.gov/31934590/>.
59. Lin C, Chao H, Li Z, Xu X, Liu Y, Bao Z, et al. Omega-3 fatty acids regulate NLRP3 inflammasome activation and prevent behavior deficits after traumatic brain injury. *Exp Neurol.* 2017; [cited 2020 Nov 11]. Available from: <https://pubmed.ncbi.nlm.nih.gov/28077335/>.
60. Wang J, Doré S. Inflammation after intracerebral hemorrhage. *J Cereb Blood Flow Metab Off J Int Soc Cereb Blood Flow Metab.* 2007;27(5):894–908. <https://doi.org/10.1038/sj.jcbfm.9600403>.
61. Lekic T, Manaenko A, Rolland W, Krafft P, Peters R, Hartman R, et al. Rodent neonatal germinal matrix hemorrhage mimics the human brain injury, neurological consequences, and post-hemorrhagic hydrocephalus. *Exp Neurol.* 2012;236(1):69–78. <https://doi.org/10.1016/j.expneurol.2012.04.003>.

Publisher's Note

Springer Nature remains neutral with regard to jurisdictional claims in published maps and institutional affiliations.

Ready to submit your research? Choose BMC and benefit from:

- fast, convenient online submission
- thorough peer review by experienced researchers in your field
- rapid publication on acceptance
- support for research data, including large and complex data types
- gold Open Access which fosters wider collaboration and increased citations
- maximum visibility for your research: over 100M website views per year

At BMC, research is always in progress.

Learn more biomedcentral.com/submissions

